Mon. Not. R. Astron. Soc. **395,** 1925–1933 (2009) doi:10.1111/j.1365-2966.2009.14699.x

Interpreting the transmission windows of distant quasars

A. Maselli,[1⋆] A. Ferrara[2] and S. Gallerani[3,4]

[1]*Max-Planck-Institut für Astrophysik, Karl-Schwarzschild Str. 1, 85748 Garching, Germany*
[2]*Scuola Normale Superiore, Piazza dei Cavalieri 7, 56126 Pisa, Italy*
[3]*Institute of Physics, Eötvos University, Pazmany P. s. 1/A, 1117 Budapest, Hungary*
[4]*Osservatorio Astrofisico di Roma, Via di Frascati 33, 00040 Monte Porzio Catone, Italy*

Accepted 2009 February 24. Received 2009 February 24; in original form 2008 April 23

ABSTRACT

We propose the apparent shrinking criterion (ASC) to interpret the spatial extent, $R_{\rm w}$, of transmitted flux windows in the absorption spectra of high-z quasars. The ASC can discriminate between the two regimes in which $R_{\rm w}$ corresponds either to the physical size, $R_{\rm H\,II}$, of the quasar H II region or to the distance, $R_{\rm w}^{\rm max}$, at which the transmitted flux drops to $=0.1$ and a Gunn–Peterson (GP) trough appears. In the first case [H II region (HR) regime], one can determine the intergalactic medium mean H I fraction, $x_{\rm HI}$; in the second [proximity region (PR) regime], the value of $R_{\rm w}$ allows one to measure the local photoionization rate and the local enhancement of the photoionization rate, $\Gamma_{\rm G}$, due to nearby/intervening galaxies. The ASC has been tested against radiative transfer+smoothed particle hydrodynamics numerical simulations, and applied to a sample of 15 high-z ($z > 5.8$) quasar spectra. All sample quasars are found to be in the PR regime; hence, their observed spectral properties (inner flux profile, extent of transmission window) cannot reliably constrain the value of $x_{\rm H\,I}$. Four sample quasars show evidence for a local enhancement (up to 50 per cent) in the local photoionization rate possibly produced by a galaxy overdensity. We discuss the possible interpretations and uncertainties of this result.

Key words: radiative transfer – methods: numerical – intergalactic medium – quasars: general – cosmology: theory – large scale structure of Universe.

1 INTRODUCTION

All high-redshift quasar spectra with a complete Gunn–Peterson (GP) trough (Gunn & Peterson 1965) exhibit transmitted flux in an extended region between the quasar redshift and the red side of the GP trough (Fan et al. 2006, hereafter F06). These transmission windows provide a powerful, and so far unique, probe of the physical state of the intergalactic medium (IGM) beyond redshift $z > 5.7$, where the onset of the GP trough erases the information encoded in the Lyα forest.

The detection of transmitted flux at such high redshift provides a solid evidence for a reduced neutral hydrogen fraction ($x_{\rm H\,I}$) within distances of several physical Mpc[1] from the quasar (F06). Such H I decrease can be attributed to the locally enhanced photoionization rate produced by the quasar ultraviolet radiation. However, the physical interpretation of such transmission windows in terms of the IGM properties is not straightforward. Are these transmission windows the spectral counterparts of quasar H II regions (HR), with the red side of the GP trough corresponding to the location of the quasar ionization front? Or are they instead of proximity regions (PR) resulting from the reduced optical depth in the vicinity of a quasar whose H II region extends further into the IGM? We will refer to these two interpretations as the HR and PR regime, respectively. It has been demonstrated that both regimes can be used to reproduce the observed spectra, depending on the assumed quasar luminosity and lifetime, and the ionization and thermal state of the surrounding IGM [(Bolton & Haehnelt 2007b; Maselli et al. 2007, hereafter M07; Wyithe, Bolton & Haehnelt 2008, hereafter W08).

Previous studies have shown that under the assumption of the HR regime, the relatively small extent of the observed transmission windows detected in current data would imply a significant neutral hydrogen fraction still present at $z \approx 6$, that is $x_{\rm H\,I} > 0.1$ (Wyithe & Loeb 2004; Wyithe, Loeb & Carilli 2005; F06). These results are supported by independent analysis which do not explicitly assume the HR regime, based either on fitting the probability distribution function (PDF) of the Lyα optical depth, τ, within the transmission windows (Mesinger & Haiman 2007), or on the comparison of Lyα and Lyβ absorption spectra (Mesinger & Haiman 2004). However, it is difficult to reconcile these results with the analysis of dark gaps in quasars/gamma-ray bursts absorption spectra (Gallerani et al. 2008a,b), as well as with other independent probes of the hydrogen reionization history, as the Lyman Alpha Emitters surveys (e.g. Malhotra & Rhoads 2006; Dawson et al. 2007), and the integrated electron scattering optical depth measured by the *Wilkinson Microwave Anisotropy Probe* 5 (*WMAP*5) data release (Komatsu et al. 2009). All these studies suggest $x_{\rm H\,I} \ll 1$ at $z \approx 6$ and are consistent with the detection of transmitted flux in

⋆E-mail: maselli@MPA-Garching.MPG.DE
[1] Unless otherwise stated, distances are given in physical units.

high-redshift quasar spectra provided that the PR interpretation of the transmission windows applies. In this regime, the spectral extent of the windows is set by the onset of the GP trough *within* the quasar H II region. In M07, this effect has been termed *apparent shrinking*, to indicate the possibility that the physical extent of the transmitting window, $R_{\rm w}$, does not correspond to the actual H II region size, $R_{\rm H\,II}$, and in fact underestimates it.

The condition $R_{\rm w} < R_{\rm H\,II}$ is likely to arise from the combination of two factors: (i) the average IGM density gets high enough to produce complete Lyα absorption in spite of the high gas ionization level and (ii) the quasar photoionization rate drops below the minimum value required to preserve IGM transparency inside the quasar H II region.

To discriminate between the HR and PR regimes, we propose here a simple (but yet solid) criterion, the Apparent Shrinking Criterion (ASC). Such method, in addition, allows to determine $x_{\rm H\,I}(z)$ in the HR regime or to quantify local deviations from the mean cosmic photoionization rate along the line of sight (LOS) to the quasar if the PR regime holds.

2 THE APPARENT SHRINKING CRITERION

In this section, we introduce the basic idea underlying the ASC, whose main use is to discriminate between the HR and PR scenarios described above by using a given high-redshift quasar spectrum. The ASC is based on the comparison among three spatial scales: (a) the physical size of the spectral transmission window, $R_{\rm w}$, (b) the size of the quasar H II region, $R_{\rm H\,II}$, and (c) the maximum value that $R_{\rm w}$ can take, $R_{\rm w}^{\rm max}$. These are discussed separately in the following.

2.1 Size of the transmission window

$R_{\rm w}$ is a directly measurable quantity in high-z quasar spectra and it denotes the physical extent of the spectral region close to the quasar in which a non-zero flux can be detected. The determination of this quantity is affected by uncertainties on quasar redshift, $z_{\rm Q}$, and on the flux detection limit of the instrument. An additional complication is represented by the fact that the IGM transmissivity at $z \approx 6$ is a mixture of dark gaps and transmission peaks, which makes the identification of the red-side boundary of the GP trough uncertain (e.g. isolated peaks in the translucent IGM can merge with the transmission window region associated to the quasar). Here, we adopt the operational definition given in F06, which states that $R_{\rm w}$ represents the physical distance from the quasar at which, when smoothed by a top-hat filter of 20 Å, the observed flux drops below a transmission threshold of 0.1 (corresponding to a Lyα optical depth $\tau = 2.3$).

2.2 Size of the quasar H II region

$R_{\rm H\,II}$ denotes the mean radius of the quasar H II region. Due to the gas inhomogeneities and to radiative transfer effects, quasar H II regions deviate significantly (up to 15 per cent, e.g. M07) from spherical symmetry with a resulting variation of the H II region radius along different LOS (see e.g. Fig. 1). Previous studies including radiative

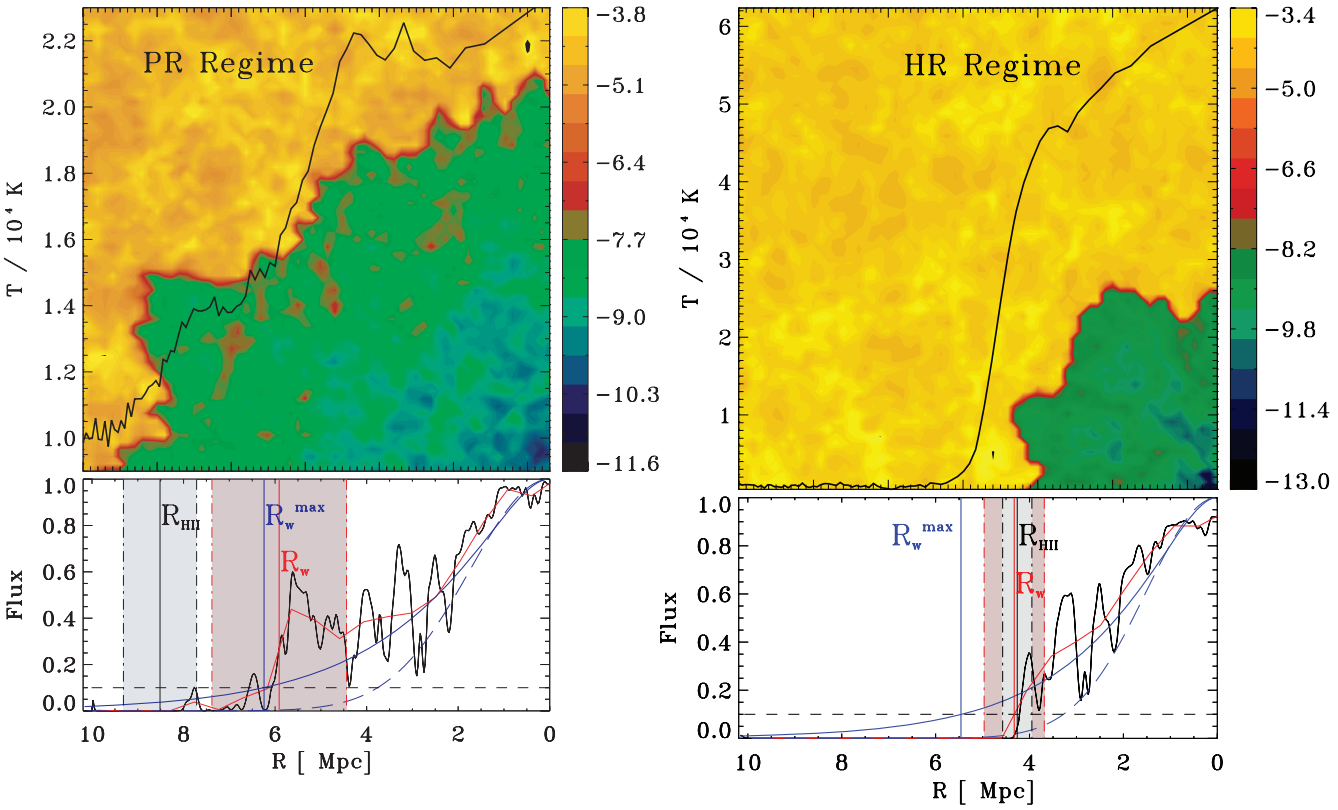

Figure 1. Simulated neutral hydrogen number density maps (upper panels, colour bars give $\log n_{\rm H\,I}$ values) and corresponding mock spectra (lower) along a typical LOS through the quasar for the PR (left-hand side, run R3) regime and HR (right-hand side, run R5). The maps are 10.1 physical Mpc on a side with the quasar located in the right-bottom corner. Overplotted are the corresponding mean temperature profiles. The lower panels show the full-resolution spectrum (black solid line), the same smoothed at 20 Å (red solid), the mean transmitted flux derived from equation (4) (solid blue) and using $F = {\rm e}^{-\tau(\Delta=1)}$ (dashed blue). The values of $R_{\rm w}$ (measured along the plotted spectrum) and of $R_{\rm w}^{\rm max}$ and $R_{\rm H\,II}$ (averaged over 1000 LOS) are shown by the vertical lines, along with the associated 1σ error (shaded band).

transfer (RT) calculations have shown that the radius of a quasar H II region expanding in a homogeneous IGM approximates well the actual mean value of $R_{\rm H\,II}$ along different lines of sight in the inhomogeneous case. Hence, we use the following expression to determine the average H II region size:

$$R_{\rm H\,II} \approx 3.3 \left(\frac{\dot{N}_\gamma}{10^{57}\ {\rm s}^{-1}} \frac{t_{\rm Q}}{10^7\ {\rm yr}}\right)^{1/3} \left(\frac{1+z}{7}\right)^{-1} x_{\rm H\,I}^{-1/3}\ {\rm Mpc}. \quad (1)$$

The above expression is valid under the additional assumption that the quasar lifetime, $t_{\rm Q} \approx 10^{7-8}$ yr, is shorter than the gas (volume-averaged) recombination time-scale,

$$t_{\rm rec}({\rm H\,I}) = 2.6 C^{-1} \left(\frac{1+z}{7}\right)^{-3}\ {\rm Gyr}, \quad (2)$$

where the clumping factor $C \equiv \langle n^2\rangle/\langle n\rangle^2 > 1$ is meant to include the effects of density inhomogeneities inside the ionized region; we have used a helium to hydrogen number ratio $y = 0.08$. Due to its low density, typical IGM recombination times are long, and exceed $t_{\rm Q}$.

2.3 Maximum size of the transmission window

A third fundamental spatial scale entering the formulation of the ASC is set by the monotonic dependence of the mean transmitted flux, $F \equiv {\rm e}^{-\tau_{\rm eff}}$, on the distance from the quasar. The detection of the GP trough in all spectra of quasars with $z > 5.7$ implies that at these redshifts the mean IGM opacity grows large enough to completely suppress transmission; due to instrumental sensitivity the detection of GP trough implies an upper limit on the mean transmitted flux of $F < 0.1$. (see e.g. F06). As a result of their large ionizing power, in the vicinity of extremely luminous quasars, the IGM opacity is suppressed with respect to average and some flux shortwards of the Lyα line can be detected. Due to the geometrical dilution of the quasar ionizing flux, F is a monotonically decreasing function of the distance from the quasar, R, and it will eventually fall below the detection threshold $F = 0.1$; at even larger distances, the quasar photoionization rate drops below the one produced by the background sources [quasi-stellar objects (QSOs) and galaxies]. Given the quasar ionizing photon rate, $\dot{N}_\gamma$, and the mean intensity of the ionizing background (or equivalently, $x_{\rm H\,I}$), one can define a radius $R_{\rm w}^{\rm max}$, as the distance from the quasar such that $F(R_{\rm w}^{\rm max}) = 0.1$, under the hypothesis that the quasar flux extends to infinity. Stated differently, $R_{\rm w}^{\rm max}$ represents the maximum spatial extent of the transmission window $R_{\rm w}$ associated to a given quasar.

How can we estimate $R_{\rm w}^{\rm max}$? Analogously to $R_{\rm H\,II}$ in equation (1), $R_{\rm w}^{\rm max}$ is calculated in the ideal case of a uniform IGM; deviations might occur due to fluctuations along different LOS, as well as to uncertainties in the modelling of the IGM and quasar properties. These effects will be quantified in the next Section.

For a uniform IGM, the mean optical depth can be expressed as a function of redshift and of the neutral hydrogen density as follows:

$$\tau = 4.25 \times 10^5 h^{-1} x_{\rm H\,I} \Delta \left(\frac{\Omega_{\rm m}}{0.26}\right)^{-0.5} \left(\frac{\Omega_{\rm b}\, h^2}{0.0241}\right) \left(\frac{1+z}{7}\right)^{3/2}, \quad (3)$$

where $\Delta \equiv \rho/\langle\rho\rangle$ denotes the gas overdensity. The mean transmitted flux is however sensitive to the PDF of the density field, $P(\Delta)$, and can be estimated as

$$F = \int P(\Delta) {\rm e}^{-\tau(\Delta)} d\Delta. \quad (4)$$

As quasars typically reside in biased (i.e. high-σ peaks) regions of the cosmic density distribution, $P(\Delta)$ might differ in their vicinity from the one describing the general IGM. Under these conditions, we do expect in particular that the peak of the PDF is shifted towards larger Δ values. In the following, though, we will neglect this bias, as both theoretical models (Barkana 2002; Wang et al. 2009) and observations (Guimarães et al. 2007) find the ambient overdensity to be significant only within a distance ($\approx$1 Mpc) much smaller than the observed values of $R_{\rm w}$: the minimum value measured to date is the one in the quasar J1623+3112 at $z = 6.22$ with $R_{\rm w} = 3.6$ Mpc.

In general, F is a function of the distance R from the quasar, through the dependence of τ on $x_{\rm H\,I}$, as in equation (3). The neutral fraction, in turn, can be derived from the condition of photoionization equilibrium at any given Δ once the local photoionization rate $\Gamma(R)$ is assigned. Close to the quasar, $\Gamma(R) \approx \Gamma_{\rm Q}(R) = \dot{N}_\gamma \bar{\sigma}_{\rm H}/4\pi R^2$, with $\bar{\sigma}_{\rm H}$ denoting the frequency-averaged photoionization hydrogen cross-section; furthermore within distances $R \approx R_{\rm H\,II}$, $\Gamma(R) \gg \Gamma_B$, the mean value in the IGM. The expression for $\Gamma_{\rm Q}$ given above neglects the flux suppression due to residual H I in the ionized region; as discussed later on, this is a good approximation supported by the results from full 3D cosmological radiative transfer simulations. An additional contribution, $\Gamma_{\rm G}$, to the total photoionization rate along the LOS can come from galaxies intervening along the line of sight.

Then the local photoionization rate can be expressed as

$$\Gamma(R) = \Gamma_B + \Gamma_{\rm G}(R) + \Gamma_{\rm Q}(R). \quad (5)$$

We initially neglect $\Gamma_{\rm G}$ and assume that $\Gamma_{\rm Q}(R)$ extends to infinity (i.e. with no truncation at the H II region ionization front whose location is unknown), and discuss the implications of such assumption in Section 4.

In summary, the estimate of the $R_{\rm w}^{\rm max}$ value associated to a given quasar requires an a priori knowledge of $\dot{N}_\gamma$, Γ_B and of the mean IGM temperature, T, which enters the determination of $x_{\rm H\,I}$ (and τ, see equation 3) via the H II recombination rate. We discuss the choice of these quantities and the associated uncertainties in Section 3. Once these quantities are fixed, $R_{\rm w}^{\rm max}$ can be estimated from photoionization equilibrium, and by requiring that $F(R_{\rm w}^{\rm max}) = 0.1$. From the analysis of RT calculations, it appears that photoionization equilibrium is a good approximation in the cases of interest. Note that $R_{\rm w}^{\rm max}$ is univocally determined by such a procedure, $\tau(R)$ being a monotonically increasing function of R as a consequence of the geometrical dilution of the quasar ionizing flux.

2.4 Formulating the ASC

Now that we have all the necessary definitions at hand, we can describe the formulation of the ASC. As anticipated above, the ASC is based on the comparison between $R_{\rm H\,II}$ and $R_{\rm w}^{\rm max}$.

The first case, $R_{\rm H\,II} > R_{\rm w}^{\rm max}$, corresponds to the PR scenario, i.e. a situation in which the quasar photoionization rate is too low to keep the gas sufficiently transparent within its own H II region. Under these conditions, the measured size of the transmission window will be equal to its theoretically determined value, $R_{\rm w} = R_{\rm w}^{\rm max}$, within uncertainties. It has already been shown that this situation is likely to occur in an ionized universe where quasar H II regions can expand several tens of Mpc into the IGM (Bolton & Haehnelt 2007b; M07), albeit it could also be found in an almost neutral gas provided that the quasar luminosity and lifetime are large enough to power a rapid growth of $R_{\rm H\,II}$.

If instead $R_{\rm H\,II} < R_{\rm w}^{\rm max}$ (HR regime), the extent of the transmission window is set by the size of the H II region, that is by the sharp $x_{\rm H\,I}$ discontinuity at the location of the ionization front. In this case $R_{\rm w} = R_{\rm H\,II}$: by construction, $R_{\rm w}^{\rm max}$ represents the upper limit to $R_{\rm w}$

Table 1. Tests of the ASC with simulations.

Run	$\dot{N}_{\gamma,57}$	$x_{\rm H\,I}$	Γ_B (10^{-13} s^{-1})	$t_{\rm Q}$ (10^7 yr)	$R_{\rm w}^{\rm max}$ (Mpc)	$R_{\rm w}$ (Mpc)	$R_{\rm H\,II}$ (Mpc)	Regime
R1	0.56	0.1	1.25×10^{-3}	1	2.51 (2.96)	2.74 ± 0.96	5.32 ± 0.61	PR
R2	0.56	$10^{-4.2}$	0.8	1	2.30 (2.43)	2.74 ± 1.60	–	PR
R3	2	0.1	1.25×10^{-3}	1	4.83 (5.35)	5.50 ± 1.47	8.51 ± 0.80	PR
R4	2	$10^{-4.2}$	0.8	1	4.51 (4.93)	5.66 ± 1.86	–	PR
R5	2	1	0.0	1	3.4 (4.7)	3.70 ± 0.64	4.26 ± 0.31	HR
R6	2	1	0.0	2	4.2 (5.7)	4.55 ± 0.89	5.39 ± 0.42	HR

obtained by assuming that quasar ionizing flux extends to infinity. The HR regime usually occurs when $x_{\rm H\,I}$ is large (i.e. small $R_{\rm H\,II}$) and the quasar ionizing flux is suppressed abruptly while still dominant over the ultraviolet background (UVB). If the HR regime holds, the measured value $R_{\rm w}$ gives an estimate of $x_{\rm H\,I}$ via equation (1) as first proposed by Wyithe & Loeb (2004). It is worth stressing that, by their own operational definition, the PR and HR regimes are not associated to a particular phase of the reionization process.

Note that, according to our definition, it is always $R_{\rm w}^{\rm max} \geq R_{\rm w}$, within errors. However, $R_{\rm w}^{\rm max}$ is determined under the assumption that $\Gamma_{\rm G} = 0$, that is neglecting a possible contribution to Γ by sources other than the quasar and the UVB. This might well not be the case. However, it is easy to isolate the effects of contributing sources (most likely galaxies) along the LOS which would be signalled by a larger than expected value $R_{\rm w} > R_{\rm w}^{\rm max}$. In this case, one would conclude that $\Gamma_{\rm G} \neq 0$; in addition, it will be also possible to obtain a quantitative estimate of such contribution by using equations (3)–(5) and further imposing that $F(R_{\rm w}) = 0.1$.

The application of the ASC will allow us to decide between the following possibilities: if $R_{\rm w} \geq R_{\rm w}^{\rm max}$ the PR regime applies and no constraints can be put on $x_{\rm H\,I}$; if moreover $R_{\rm w} > R_{\rm w}^{\rm max}$ this implies a non-vanishing contribution of galaxies to the local photoionization rate, $\Gamma_{\rm G} \neq 0$. If instead $R_{\rm w} < R_{\rm w}^{\rm max}$, the HR regime applies, $R_{\rm H\,II} \approx R_{\rm w}$, and $x_{\rm H\,I}$ can be constrained.

3 THE ERROR BUDGET

In this section, we discuss and quantify the various uncertainties involved in the determination of the three characteristic scales entering the ASC, together with their associated error sources.

3.1 $R_{\rm H\,II}$

$R_{\rm H\,II}$ denotes the average extent of the quasar H II region and consequently the uncertainty on this quantity is associated to fluctuations in the density field and radiative transfer effects (e.g. shadowing, filtering and self-shielding) which distort the shape of the quasar H II region; the extent of the H II region is then direction-dependent. The amplitude of this effect can be estimated only with the support of 3D numerical simulations.

We have then performed a set of dedicated 3D radiative transfer simulations which follow the expansion of the H II region in a cosmological density field for different quasars and IGM parameters, as described in more details in Section 4. We use the outputs of such simulations to quantify the relative error $\Delta R_{\rm H\,II}/R_{\rm H\,II}$. For each simulation, we have drawn 1000 LOS towards the quasar and on each LOS we have estimated $R_{\rm H\,II}$ as the distance R at which $\partial x_{\rm H\,I}/\partial R > 100$. $\Delta R_{\rm H\,II}$ is quantified as the 1σ dispersion of the $R_{\rm H\,II}$ distribution derived as above.

Table 1 reports $R_{\rm H\,II}$ and the associated error for various simulation runs.[2] We find the relative error on $R_{\rm H\,II}$ to be confined in the extremely narrow range 0.07–0.11, despite the wide range covered by the average extents of the H II regions which result from spanning over the values allowed for the simulation parameters ($\dot{N}_\gamma$, $x_{\rm H\,I}$, $t_{\rm Q}$).

3.2 $R_{\rm w}$

The extent of the transmission window is an observable quantity in the spectra of high-z quasars whose estimate is derived from the measurement of the quasar redshift ($z_{\rm Q}$) and the onset of the GP trough ($z_{\rm w}$) along a given LOS. The accuracy of the quasar redshift depends on the line indicators available. The most accurate determination relies on CO rotational transition lines from the host galaxy. Only for two of the high-z quasars analysed (see Section 5) CO detection is currently available: J1148+5251 (Bertoldi et al. 2003) and J0927+2001 (Carilli et al. 2007); for these cases redshifts are measured with an uncertainty $\Delta z_{\rm Q} < 0.0001$. The next accurate indicator for systemic quasars redshift is the Mg II line which, despite being a broad line, allows accuracy of the order of $0.002 < \Delta z_{\rm Q} < 0.004$ (Richards et al. 2002). However the Mg II transition line has a rest-frame wavelength of 2800 Å, so that at $z \approx 6$ it is shifted to roughly 2 μm, thus requiring infrared spectroscopy which is not always available. When neither CO nor Mg II detections are available the redshift is measured via the Lyα line which has an associated error of the order of $\Delta z_{\rm Q} \approx 0.02$. In the quasars list reported in Table 1, the redshifts are tagged with a letter specifying the line indicator used.

Extracting an accurate measurement of $z_{\rm w}$ from the observed spectra is also not trivial, as already discussed in Section 2.1. As mentioned there, we adopt the operational definition given in F06, i.e. $z_{\rm w}$ is taken as the redshift corresponding to the first pixel, moving away from the quasar location, at which the flux smoothed by a top-hat filter of 20 Å drops below the threshold $F = 0.1$. At $z \approx 6$, 20 Å correspond roughly to $\Delta z_{\rm w} \approx 0.02$. We take the latter as a measure of the error on $z_{\rm w}$.

Aside from the intrinsic error associated to the $R_{\rm w}$ measurement along the observed LOS, the uncertainty on $R_{\rm w}$ must take into account the dispersion along different LOS towards the same target quasar. Analogously to the case of $R_{\rm H\,II}$, quantifying such an error requires the support of 3D numerical simulations. We have used the same sample of LOS used for the $\Delta R_{\rm H\,II}$ determination, to extract the mock spectrum and the associated value of $R_{\rm w}$ for each LOS (the details of such procedure are given in Section 4). The average $R_{\rm w}$ values found for the various simulations are given in Table 1 together with the associated 1σ dispersion of the sample.

[2] For runs R2 and R4, these values are not given as these cases correspond to an initially highly ionized IGM in which the quasar H II region becomes larger than the computational volume.

As already pointed out in our previous work (M07), $R_{\rm w}$ fluctuations along different LOS are significantly larger with respect to the $R_{\rm H\,II}$ ones: this is due to the fact that $R_{\rm w}$ depends on the Lyα optical depth which is extremely sensitive to tiny fluctuations of $x_{\rm H\,I}$, while $R_{\rm H\,II}$ is set by the sharp $x_{\rm H\,I}$ transition occurring at the ionization front. Differently from $R_{\rm H\,II}$, $R_{\rm w}$ has a stronger dependence on the physical state of the gas in which the quasar is embedded. We find $\Delta R_{\rm w}/R_{\rm w}$ values ranging from 0.17 to 0.58, with the general trend of $\Delta R_{\rm w}/R_{\rm w}$ increasing with decreasing values of the ratio $\dot{N}_\gamma/\Gamma_B$. This behaviour is determined by the fact that $R_{\rm w}$ gets smaller for smaller $\dot{N}_\gamma$, while for higher Γ_B values the dispersion, $\Delta R_{\rm w}$, increases as a consequence of a more sensitive response to density fluctuations. Given the limited a priori knowledge of $\dot{N}_\gamma/\Gamma_B$ in this study, we assume the average value $\langle \Delta R_{\rm w}/R_{\rm w}\rangle = 0.3$.

3.3 $R_{\rm w}^{\rm max}$

As described in Section 2.3, the determination of $R_{\rm w}^{\rm max}$ involves the assumption of the following parameters: the quasar intrinsic luminosity, $\dot{N}_\gamma$, the gas temperature, T, and the UVB photoionization rate, Γ_B.

Quasar luminosities are commonly estimated by converting the observed magnitudes in number of ionizing photons emitted per unit time. Such a procedure requires the assumption of a specific template for the quasar intrinsic spectrum, which is poorly constrained for high-redshift quasars. In principle, each quasar is characterized by its own spectral energy distribution and it would be possible to associate at each observed object a power law with a specific spectral index inferred from infrared data, which however are not always available for the current analysis. In the current work, we derive $\dot{N}_\gamma$ by using the measured absolute magnitude M_{1450} at 1450 Å, and assuming the spectral template by Telfer et al. (2002). This is the composite spectrum of lower redshift quasars ($z \lesssim 3.7$), which is well fitted by a double power-law with a break close to the Lyα line at $\lambda = 1280$ Å and spectral indexes $\alpha_{\rm EUV} = -1.76$ and $\alpha_{\rm NUV} = -0.69$. As done in Yu & Lu (2005), we take into account the uncertainty associated to the template by considering also the Telfer double power-low fits to the subsamples of radio-quiet and radio-loud quasars, which has spectral indexes ($\alpha_{\rm EUV}^{\rm rl} = -1.96$, $\alpha_{\rm NUV}^{\rm rl} = -0.67$) and ($\alpha_{\rm EUV}^{\rm rq} = -1.57$, $\alpha_{\rm NUV}^{\rm rq} = -0.72$), respectively.

The IGM temperature as well as the UVB photoionization rate, Γ_B, is also poorly constrained at high redshift. Nevertheless, the statistical analysis of the Lyα forest detected in high-z quasar spectra, as well as both analytic and numerical theoretical models of the reionization process, allows to bracket the above quantities into a relatively narrow range of possible values (e.g. Choudhury & Ferrara 2006; Gallerani et al. 2008a). In the application of the ASC to the observed high-z quasar spectra presented in this paper and discussed in detail in Section 5, we assume Γ_B to evolve according to the early reionization model (ERM) developed by Gallerani et al. (2008a). In such model, reionization completes at $z_{rei} \approx 7$ after an extended partial ionization phase, necessary to recover the recent determination of the electron scattering optical depth found from WMAP5 data (Dunkley et al. 2009). Such model also simultaneously accounts for most of the available data including Lyα/Lyβ GP opacity, Lyman Limit Systems, cosmic star formation history, the number density of high-redshift sources, and the luminosity functions of Lyman Alpha Emitters at $4.5 < z < 6.6$ (Dayal, Ferrara & Gallerani 2008). Moreover, the UVB photoionization rate predicted by the ERM is consistent with the results by Bolton et al. (2005) and Bolton & Haehnelt (2007b) in the range $4 < z < 6$. At $z \approx 6$, the latter authors provide a solid upper limit $\Gamma_B \leq 0.34 \times 10^{-12}$ s^{-1}, which we take here to quantify the uncertainties on $\Gamma_B(z)$. Smaller values of Γ_B do not affect significantly the $R_{\rm w}^{\rm max}$ estimate, due to the fact that at the characteristic distances involved (several physical Mpc) the local photoionization rate is still dominated by the quasar ionizing flux.

The ERM prescribes IGM temperatures in the range $T = (1 \pm 0.5) \times 10^4$ K. We take $T = (1.5 \pm 0.5) \times 10^4$ K to allow for a possible local boost induced by the quasar. Note in fact that, as seen from our RT simulations presented in Fig. 1, the extra heating provided by the quasar can raise the gas temperature above 2×10^4 K only for the case in which the quasar ionization front expands in a completely neutral gas, a possibility already excluded by various high-z experiments (see Introduction).

4 TESTING THE ASC WITH SIMULATIONS

Before applying the ASC to observations we have tested it through a set of numerical simulations which combine smoothed particle hydrodynamics (SPH) (Springel & Hernquist 2003) and full 3D radiative transfer (RT) calculations performed with CRASH (Maselli, Ferrara & Ciardi 2003). These tests are meant to check the validity of the ASC and more precisely to verify that the semi-analytic method devised to determine $R_{\rm w}^{\rm max}$ gives reliable results. If so, when applied to the synthetic spectra extracted from the simulations, the ASC should be able to correctly predict the physical regime (PR or HR) prevailing in the computational volume.

The simulations setting is similar to the one described in M07, to which we defer the reader for details. The two main differences here are the inclusion of helium physics and the newly developed 'coloured packets' RT algorithm (Maselli, Ciardi & Kanekar 2008) which allows to more reliably compute the effects of hard spectrum sources. This allows to extract mock spectra with improved precision. Using the SPH density field at $z = 6.093$ as an input, we have run CRASH for different combinations of the free parameters ($\dot{N}_\gamma, t_{\rm Q}, x_{\rm H\,I}$). The set of simulations performed is listed in Table 1, where we give the free parameters adopted for each run, identified by the name in first column, along with values of $R_{\rm w}^{\rm max}$, $R_{\rm w}$, their associated 1σ errors and the corresponding regime determined from the simulations. From each simulation, we build synthetic Lyα absorption spectra along 1000 LOS through the box, smooth the spectra at 20 Å as described in M07, and derive the average value of $R_{\rm w}$. The corresponding $R_{\rm w}^{\rm max}$ is evaluated following the procedure described in Section 2.3 adopting the values of Γ_B and $\dot{N}_\gamma$ of the specific RT run, as well as the numerically computed/LOS-averaged neutral hydrogen density and temperature profiles. Due to the inhomogeneities of the density field and to RT effects, the quasar H II regions found in our numerical simulations are not spherical, with significant scatter of the H II region size along different directions (e.g. see Fig. 1). We then compute $R_{\rm H\,II}$ by averaging the value over all the LOS. For all the simulated configurations in which the H II region is confined inside the computational volume (R1, R3, R5, R6), we find that the average values of $R_{\rm H\,II}$ are consistent with the approximated values given by equation (1) within few per cent. This result shows photoionization equilibrium, assumed in the calculation of $R_{\rm w}^{\rm max}$ (Section 2.3), to be an excellent approximation.

Two examples of PR (left-hand side) and HR (right-hand side) regimes are shown in Fig. 1, taken from the runs R3 and R5, respectively. The maps show H I number density cuts in a region of 50 h^{-1} Mpc (comoving) on a side with the quasar located in the right-bottom corner. Overplotted in the maps is the averaged temperature profile within the same region. In the corresponding bottom panels of the same figure, the black (red) solid lines show the

full-resolution (20 Å smoothed) absorption spectrum along a random LOS to the quasar, from which we determine $R_{\rm w}$ according to the operational definition given in Section 2.3. The mean transmitted flux derived from equation (4) is shown by the solid blue lines, while the dashed curves represent the mean transmitted flux for the case of an homogeneous density field at the mean density, that is $P(\Delta) = \delta(1)$.

By comparing the analytical transmitted fluxes curves to the mock spectra, it is evident that to correctly compute the IGM mean opacity at high z, the proper PDF of the density field, and particularly of underdense regions, must be taken into account. At high redshift, in fact, $\tau(\Delta = 1)$ grossly overestimates the effective opacity. This occurs because fluctuations above a certain overdensity threshold, $\Delta_{\rm th}$, start to become opaque due to the progressive increase of the average cosmic density with z, which prevents the gas at $\Delta \geq \Delta_{\rm th}$ to remain sufficiently ionized to be transparent. The value of $\Delta_{\rm th}$ decreases gradually with redshift and becomes <1 at $z \approx 6$.

Fig. 1 illustrates visually the relation among $R_{\rm w}$, $R_{\rm w}^{\rm max}$ and $R_{\rm H\,II}$ as a function of the different physical conditions of the gas in the two regimes. Note that in these plots, the mock spectra as well as $R_{\rm w}$ are computed along a single random LOS; $R_{\rm w}^{\rm max}$ is determined analytically, and $R_{\rm H\,II}$ is the average value over all the LOS. This choice is meant to reproduce the closest analogue to the actual experiment. In the PR regime (left-hand panel), we find $R_{\rm w}^{\rm max} \approx R_{\rm w}$ as expected, implying, according to the ASC, that the quasar H II region should be larger, $R_{\rm H\,II} > R_{\rm w}^{\rm max} \approx R_{\rm w}$. This prediction is confirmed, as seen from the position of $R_{\rm H\,II}$ shown in the panel. On the contrary, in the situation in which $R_{\rm w}^{\rm max} > R_{\rm w}$, as in the right-hand panel corresponding to the HR regime, $R_{\rm w}$ truly measures the H II region radius. Again the simulation results confirm the validity of the ASC prediction. In this case by inverting equation (1), we obtain a (nominal) value $x_{\rm H\,I} = 0.89 \pm 0.2$, consistent with the neutral hydrogen fraction, $x_{\rm H\,I} = 1$, imposed as initial condition in this run.[3]

More systematic tests of the ASC have been envisaged with the set of simulations reported in Table 1, which span the allowed values of the free parameters of the problem ($\dot{N}_\gamma$, $t_{\rm Q}$, $x_{\rm H\,I}$). For each run, we give here the values of $R_{\rm w}^{\rm max}$, $R_{\rm w}$, and their associated 1σ error (see discussion in Section 3). We provide two different estimates for $R_{\rm w}^{\rm max}$: the first (fiducial) is obtained by using the average $n_{\rm H\,I}$ profiles extracted from the RT simulations, the second, $R_{\rm w}^{\rm max}$ $(noRT)$ (in brackets) by neglecting RT effects. In this latter case, $x_{\rm H\,I}$ inside the H II region is calculated by assuming that the SPH simulated density field is at photoionization equilibrium with the *unattenuated* quasar flux plus background: this method does not account for (i) residual H I inside the H II region and (ii) the drop of the quasar flux beyond the ionization front.

From the data in Table 1, we find that $R_{\rm w}^{\rm max}$ is within the $R_{\rm w}$ range derived from the mock spectra; $R_{\rm w}^{\rm max}$ $(noRT)$ is in agreement with $R_{\rm w}$ for PR cases, but it exceeds $R_{\rm w}$ for the R5 and R6 (HR regime) runs, as expected from the ASC: $R_{\rm w}$ in these cases corresponds to the H II region radius (equation 1), a result confirmed by the analysis of these simulation outputs.

The comparison between the fiducial and no-RT (bracketed) $R_{\rm w}^{\rm max}$ values shows furthermore that RT effects associated to the internal residual H I opacity can be safely neglected in the calculation of $R_{\rm w}^{\rm max}$, whereas the flux drop occurring in the HR regime beyond the ionization front cannot be disregarded. Stated in a different manner, the power of the ASC to discriminate between PR and HR regimes exploits the strong flux drop-off taking place at the H II region ionization front.

[3] Relativistic effects related to finite light propagation on the apparent shape of the H II regions do not affect the direction along the LOS and thus the validity of the ASC which applies to single LOS.

5 APPLICATION TO DATA

Having successfully tested the ASC, we apply it to a sample of high redshift quasar spectra taken from F06. The selected quasars name, redshift, ionizing photon rate, observed $R_{\rm w}$ value along with our fiducial $R_{\rm w}^{\rm max}$ estimate, are reported in Table 2. The redshift values are taken from F06, unless measurements of low-ionization lines like Mg II (Jiang et al. 2007; Kurk et al. 2007) or of CO rotational lines (J0927+2001 from Carilli et al. 2007; J1148+5251 from Bertoldi et al. 2003) do exist. The QSO ionizing rates have been derived from their magnitudes, as discussed in Section 3.3 assuming the Telfer composite spectrum. The $R_{\rm w}^{\rm max}$ values are determined from the semi-analytic procedure described in Section 3.3 and adopting the overdensity PDF extracted from the SPH simulation described in Section 4. In addition, Γ_B and the IGM temperature, T, are assumed to evolve according to the ERM developed by Gallerani et al. (2008a). The details of the above models have been given in Section 3.3, where we also discuss the uncertainties associated with Γ_B and T.

Fig. 2 shows the comparison between $R_{\rm w}$ and $R_{\rm w}^{\rm max}$ for the quasar sample in Table 2. As discussed in Section 3.2, the errors on $R_{\rm w}$ are dominated by the uncertainty associated to the dispersion along different LOS. The $R_{\rm w}^{\rm max}$ values shown in Fig. 2 by the black squares are obtained by adopting an IGM temperature $T = 1.5 \times 10^4$ K. The shaded region represents the error on $R_{\rm w}^{\rm max}$ associated to the uncertainties on the temperature and on the spectral template: the upper (lower) solid line connects the values associated with the larger (smaller) photoionization rates corresponding to the double power-law fitting the radio-quiet (radio-loud) composite spectrum, and to the upper (lower) limit on the temperature consistent with the ERM, $T = 2 \times 10^4$ K ($T = 10^4$ K). Note that higher temperatures at fixed density yield lower optical depths, larger transmitted fluxes and consequently higher $R_{\rm w}^{\rm max}$ values. Fig. 2 also shows the $R_{\rm w}^{\rm max}$ values obtained for the fiducial T and $\dot{N}_\gamma$ values, but with different assumptions on Γ_B: we consider the extreme cases of (i) a constant Γ_B equal to the upper limit given by Bolton & Haehnelt 2007b of $\Gamma_{B,-12} = 0.34$ (dashed-black line), and (ii) $\Gamma_B = 0$ (dotted-black line). The small differences between these two extreme cases demonstrate that uncertainties in the intensity of the UVB do not sensibly affect the ASC. This results from the fact that, at the scales relevant to ASC, the local ionization rate is dominated by the quasar flux, that is $\Gamma \simeq \Gamma_{\rm Q}$.

Fig. 2 represents the central result of this paper, that is the application of the ASC to a sample containing the most distant quasars, and it allows us to draw a number of interesting conclusions. None of the analysed quasars satisfies the condition $R_{\rm w} < R_{\rm w}^{\rm max}$ (within uncertainties), indicating that all sample QSOs are in the PR regime. As a consequence, current observations cannot provide reliable estimates of the IGM ionization state by studying their H II region.

Secondly, we find $R_{\rm w} > R^{\rm max}$ for the quasar J1602+4228 at $>2\sigma$ significance level, and for the quasars J1436+5007, J1411+1217, J1623+3112 at a lower significance level. According to the ASC this occurrence signals a locally enhanced photoionization rate. As discussed in Section 2.4, this could be due to either a higher than average number density of galaxies clustered around the quasar or a local enhancement of more distant galaxies along the observed LOS, but not directly associated to the overdensity in which the

Table 2. Quasar sample. Quasar redshifts are tagged according to the spectral lines used for their measurement and to reference works as follows: (a) CO (Carilli et al. 2007), (b) Lyα (F06), (c) Mg II (Jiang et al. 2007), (d) Mg II (Kurk et al. 2007), (e) CO (Bertoldi et al. 2003) and (f) (White et al. 2003).

Quasar	z_Q	z_w	M_{1450}	$\dot{N}_{\gamma,57}$ Fiducial	$\dot{N}_{\gamma,57}$ Radio loud	$\dot{N}_{\gamma,57}$ Radio quiet	R_w	R_w^{max}
$J0927+2001$	5.77^a	5.700^b	-26.78	1.00	0.85	1.15	4.96	4.45
$J0002+2550$	5.80^b	5.650^b	-27.70	2.33	1.98	2.68	10.68	7.15
$J0836+0054$	5.81^c	5.721^d	-27.83	2.63	3.02	2.23	6.24	7.55
$J1436+5007$	5.83^b	5.720^b	-26.51	0.79	0.90	0.66	7.69	3.75
$J0005-0006$	5.85^d	5.771^d	-26.42	0.72	0.82	0.61	5.45	3.55
$J1411+1217$	5.93^c	5.823^d	-26.70	0.93	1.07	0.80	7.20	3.85
$J0818+1722$	6.00^b	5.920^b	-27.37	1.72	1.98	1.46	5.22	4.95
$J1306+0356$	6.01^d	5.916^d	-27.14	1.39	1.60	1.18	6.13	4.45
$J1137+3549$	6.01^b	5.910^b	-27.08	1.32	1.51	1.12	6.53	4.25
$J1630+4012$	6.05^b	5.980^b	-26.11	0.54	0.62	0.46	4.48	2.65
$J1602+4228$	6.07^b	5.950^b	-26.82	1.04	1.19	0.88	7.70	3.65
$J1250+3130$	6.13^b	6.030^b	-27.11	1.35	1.56	1.15	6.25	4.05
$J1623+3112$	6.25^c	6.160^f	-26.67	0.90	1.04	0.77	5.39	3.05
$J1030+0524$	6.31^d	6.217^d	-27.15	1.41	1.62	1.20	5.52	3.65
$J1148+5251$	6.42^e	6.325^f	-27.82	2.60	2.99	2.22	5.37	4.75

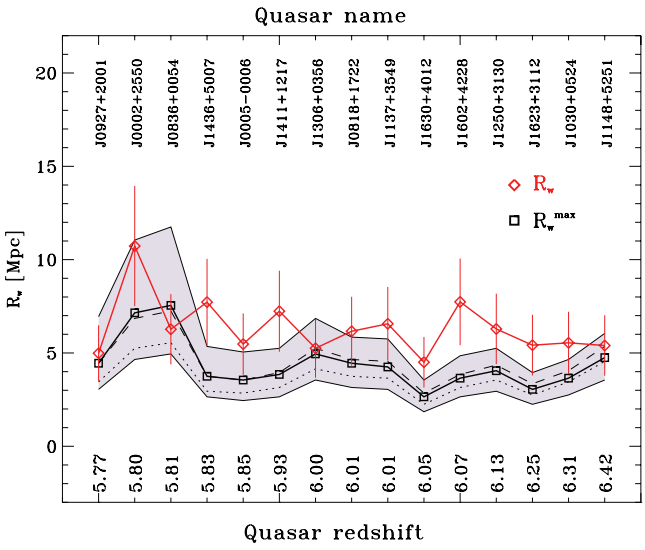

Figure 2. Comparison between the observed R_w and corresponding values of R_w^{max} for the sample quasars listed in Table 2. Red diamonds show the measured R_w, black squares are the values obtained for R_w^{max}. The shaded region accounts for the errors associated with the uncertainties in the gas temperature and quasar template; the dashed (dotted) line connects R_w^{max} values obtained assuming $\Gamma_{B,-12} = 0.34$ ($\Gamma_B = 0$), at fixed IGM temperature ($T = 1.5 \times 10^4$) and Telfer quasar template.

quasar is located. Another possibility is that the contribution to the local photoionization rate due to the galaxies around the quasar is increased by the enhanced mean free path produced by the quasar ionizing flux. In order to decide among these possibilities accurate spectroscopic redshift determinations from deep galaxy surveys of the quasars fields would be necessary, which unfortunately are not available yet.

Independently of its origin, the ASC allows us to directly infer the amplitude of Γ_G at R_w by progressively increasing $\Gamma(r)$ (equation 5) until the condition $R_w^{max} = R_w$ is met. Following this procedure, we obtain: $\Gamma_G^{J1436} = 1.63 \times 10^{-13}$ s^{-1}, $\Gamma_G^{J1411} = 1.85 \times 10^{-13}$ s^{-1}, $\Gamma_G^{J1602} = 2.38 \times 10^{-13}$ s^{-1} and $\Gamma_G^{J1623} = 3.09 \times 10^{-13}$ s^{-1}. These values are comparable to the average intensity of the UVB at the same redshift: $0.35 < \Gamma_G/\Gamma_B < 0.85$. Furthermore, for all these four QSOs, we find that Γ_G is comparable or exceeds Γ_Q at R_w, with derived values of the ratio $\Gamma_G/\Gamma_Q = 1.25, 1.05, 1.49, 1.02$. Such ionizing photon contribution from galaxies is crucial to explain the width of the transmission windows.

6 DISCUSSION

We have proposed the Apparent Shrinking Criterion (ASC), a simple but yet robust semi-analytic method, based on the apparent shrinking effect M07, which can be applied straightforwardly to the interpretation of transmission windows in the spectra of distant quasars. The ASC is based on the comparison between three spatial scales associated with a quasar: these are $R_{H\,II}$, the average physical radius of the H II region, the extent of the transmission window detected in its spectrum, R_w, and R_w^{max}, the distance from the quasar at which the mean transmitted flux drops to $F = 0.1$ in the absence of attenuation due to either H I internal to the H II region or the ionization front of the latter.

The ASC applied to the spectra of single high-z QSOs provides a novel method to discriminate between the two scenarios previously proposed in the literature to explain the QSO transmitted flux. In the first one, the extent of the observed transmission window, R_w, is set by the sharp drop of the quasar ionizing flux at the ionization front location, so that R_w gives a measure of $R_{H\,II}$. If the quasar H II region grows large though the unattenuated/geometrically diluted quasar flux gets progressively weaker and eventually falls below the threshold necessary to keep the IGM transparent to Lyα radiation. As a result, the observed R_w saturates at the theoretically estimated upper limit R_w^{max}, independently of the actual extent of the H II region, so that $R_w \approx R_w^{max} < R_{H\,II}$. We refer to the first/second case as the H II region (HR)/PR regime, respectively. In the HR regime, one can determine $x_{H\,I}$, the IGM mean H I fraction. If the PR regime holds instead, the value of R_w can be used to constrain the local (i.e. at a distance R_w from the quasar) intensity of the ionizing radiation and indirectly infer the contribution of intervening clustered galaxies to the local photoionization rate.

As formulated in this paper, the ASC can only be applied to single objects and at the moment it is unclear whether it could be extended to get information on the average IGM properties at high redshift. At the moment, the ASC must be interpreted as a useful local test of reionization, that is in regions surrounding luminous quasars. Nevertheless, by separately collecting information from a large sample of quasars in a given redshift range, the ASC can eventually give new constraints on the global reionization history. We leave the analysis of this further extension of the ASC for future work.

The novelty introduced by the ASC is that it makes possible to assess the physical regime (HR or PR) characterizing an observed quasar. Previous works have instead focused on extracting global information on the IGM redshift evolution from generic trends in the data, for example the dependence of $R_{\rm w}$ on redshift (F06; W08), statistical fits to the $R_{\rm w}$ distribution function (Wyithe & Loeb 2004), and/or fits to the flux profiles within the transmission windows (Mesinger & Haiman 2007). The drawback of the first two approaches is that, in order to carry such studies, it is necessary to make a scaling of $R_{\rm w}$ to a reference quasar luminosity, a procedure which is valid only in the case in which the quasars are all in the HR regime. By implicitly making this assumption the information encoded in the observed spectra is degraded. The same happens in the flux profile fitting procedure, which is meant to constrain the most probable values for the triplet ($R_{\rm H\,II}$, $\dot{N}_\gamma$, $x_{\rm H\,I}$). Although in this case the hypothesis that $R_{\rm w}$ identifies the H II region radius is not made explicitly, the transmission profile shape is sensitive to the three parameters above only in the HR regime; in the PR regime the profiles are sensitive to $\dot{N}_\gamma$, but completely degenerate with $R_{\rm H\,II}$ and $x_{\rm H\,I}$.

The ASC has been extensively and successfully tested, by applying it to synthetic absorption spectra extracted from a set of state-of-the-art numerical simulations. Next, the ASC has been applied to a sample of high redshift quasar spectra taken from F06.

The main result is that all quasars in the analysed sample are found to be in the PR regime and hence their spectral observables (inner flux profile, extent of transmission windows) cannot be used to reliably constrain the value of the average IGM neutral hydrogen fraction. Nevertheless, for quasars in the PR regime the ASC offers a novel method to determine the local photoionization rate, analogous to the proximity effect at lower redshift (Bajtlik, Duncan & Ostriker 1988). As an outcome of our analysis, we find that all the observed quasar spectra considered are consistent with the ERM described in Gallerani et al. (2008a), which predicts reionization to be complete at $z \approx 7$ and thus the IGM at $z \approx 6$ to be highly ionized.

Beside these general results, we have found that four objects (J1436+5007, J1411+1217, J1602+4228 and J1623+3112) show the presence of an additional contribution, $\Gamma_{\rm G} \neq 0$, to the local photoionization rate. The origin of this extra ionizing radiation is still unclear. Such flux could be provided by (i) galaxies clustered in the biased high density regions in which quasars are expected to form, (ii) a galaxy overdensity intervening along the observed LOS to the quasar and not directly associated to the quasar overdensity, (iii) galaxies within the quasar H II region whose contribution to the photoionization rate is boosted by the quasar-enhanced mean free path of ionizing photons. For the four quasars above we found that $1.02 \leq \Gamma_{\rm G}/\Gamma_{\rm Q} \leq 1.49$, thus showing that for these cases the galaxy ionizing flux is comparable to the quasar one at $R_{\rm w}$. The interpretation of this result within structure formation scenarios might give interesting clues on the environmental impact of high-z quasars.

In the process of testing the ASC with our RT+SPH simulations, we have shown a further interesting point: a correct estimate of the IGM mean opacity at high z requires to properly weight the contribution from underdense regions with their actual PDF. At high redshift in fact, fluctuations with overdensity above a certain threshold start to become opaque due to the progressive increase of the average cosmic density with z, and hence do not contribute to transmission even if they are still highly ionized. This overdensity threshold decreases gradually with redshift and it falls significantly below unity at $z \approx 6$.

As a final remark, we emphasize that the lack of sample quasars in the H II region regime does not dismiss the potential use of quasar transmission windows to directly measure $x_{\rm H\,I}$ at $z > 6$: in fact, we do expect that with the detection of higher redshift and/or lower luminous objects expected in the near future, spectra in the HR regime will likely be found.

ACKNOWLEDGMENTS

We thank G. Worseck for useful comments, and X. Fan for providing some of the data listed in Table 2. Useful discussions with J. Bolton and T. Choudhury are acknowledged. AM is supported by the DFG Priority Program 1177. SG acknowledges the support by the Hungarian National Office for Research and Technology (NKTH), through the Polányi Program.

REFERENCES

Bajtlik S., Duncan R. C., Ostriker J. P., 1988, ApJ, 327, 570
Barkana R., 2002, MNRAS, 347, 59
Bertoldi F. et al., 2003, A&A, 409, L47
Bolton J. S., Haehnelt M. G., 2007a, MNRAS, 374, 493
Bolton J. S., Haehnelt M. G., 2007b, MNRAS, 382, 325
Bolton J. S., Haehnelt M. G., Viel M., Springel V., 2005, MNRAS, 357, 1178
Carilli C. L. et al., 2007, ApJ, 666, L9
Choudhury T. R., Ferrara A., 2006, MNRAS, 371, 55
Dayal P., Ferrara A., Gallerani S., 2008, MNRAS, 389, 1683
Dawson S., Rhoads J. E., Malhotra S., Stern D., Wang J., Dey A., Spinrad H., Jannuzi B. T., 2007, ApJ, 671, 1227
Dunkley J. et al., 2009, ApJS, 180, 306
Fan X. et al., 2006, ApJ, 132, 117 (F06)
Gallerani S., Ferrara A., Fan X., Choudhury T. R., 2008a, MNRAS, 386, 359
Gallerani S., Salvaterra R., Ferrara A., Choudhury T. R., 2008b, MNRAS, 388, L84
Guimarães R., Petitjean P., Rollinde E., Carvalho R. R., Djorgovski S. G., Srianand R., Aghaee A., Castro S., 2007, MNRAS, 377, 657
Gunn J. E., Peterson B. A., 1965, ApJ, 142, 1633
Jiang L., Fan X., Vestergaard M., Kurk J. D., Walter F., Kelly B. C., Strauss M. A., 2007, AJ, 137, 1150
Komatsu E. et al., 2009, ApJS, 180, 330
Kurk J. D. et al., 2007, ApJ, 669, 32
Malhotra S., Rhoads J. E., 2006, ApJ, 647, L95
Maselli A., Ciardi B., Kanekar A., 2008, MNRAS, 393, 171
Maselli A., Ferrara A., Ciardi B., 2003, MNRAS, 345, 379
Maselli A., Gallerani S., Ferrara A., Choudhury T. R., 2007, MNRAS, 376, L34 (M07)
Mesinger A., Haiman Z., 2004, ApJ, 611, L69
Mesinger A., Haiman Z., 2007, ApJ, 660, 923
Richards G. T., Vanden Berk D. E., Reichard T. A., Hall P. B., Schneider D. P., SubbaRao M., Thakar A. R., York D. G., 2002, AJ, 124, 1
Springel V., Hernquist L., 2003, MNRAS, 339, 312

Wang H., Mo H. J., Jing Y. P., Guo Y., van den Bosch F. C., Yang X., 2009, MNRAS, 394, 398
Telfer R. C., Zheng W., Kriss G. A., Davidson A. F., 2002, ApJ, 565, 773
White R., Becker R., Fan X., Strauss M., 2003, AJ, 126, 111, L69
Wyithe J. S. B., Loeb A., 2004, Nature, 427, 81
Wyithe J. S. B., Bolton J. S., Haehnelt M. G., 2008, MNRAS, 383, 691 (W08)
Wyithe J. S. B., Loeb A., Carilli C. L., 2005, ApJ, 628, 575
Yu Q., Lu Y., 2005, ApJ, 620, 31

This paper has been typeset from a TEX/LATEX file prepared by the author.